World Electric Vehicle Journal

MDPI

Article

Stabilization of Vehicle Dynamics by Tire Digital Control—Tire Disturbance Control Algorithm for an Electric Motor Drive System

Keizo Akutagawa [1,*] and Yasumichi Wakao [2]

[1] Bridgestone Corporation; 3-1-1 Ogawahigashi-cho, Kodaira-shi, Tokyo 187-8531, Japan
[2] Bridgestone Corporation, 1-1, Kyobashi 3-chome, Chuo-ku, Tokyo 104-8340, Japan; yasumichi.wakao@bridgestone.com
* Correspondence: keizo.akutagawa@bridgestone.com

Received: 16 April 2019; Accepted: 18 May 2019; Published: 21 May 2019

Abstract: We propose an algorithm with disturbance control for tires on electric vehicles (EVs) so as to improve the steering stability of the vehicle. The effect was validated on EVs equipped with twin independent electric motors on a skid pad. The algorithm with the disturbance controller can remove the external noise generated on tires in order to suppress the abrupt slip and micro vibration generated between the tire and road surface, especially on low friction surfaces at the critical speed of the vehicle. The effective frequency corresponded to tire scale length. The effect was verified by the fact that the hysteresis loop with control on the chart of steer angle and yaw rate showed a smaller loop than those without control. The hysteresis loop with control also appeared at the oversteering area, which can be interpreted as evidence that the algorithm can make the vehicle more stable and gain faster speed on the skid pad. It is concluded that the tire digital control works well without any information from sensors on the vehicle body and without any cooperative control between tires.

Keywords: tire; disturbance; stabilization; digital control; electric motor

1. Introduction

The international energy agency (IEA) reported on the global market trend of electric vehicles (EVs) in Global Electric Vehicle Outlook 2018 [1]. Over 1 million electric cars were sold in 2017 with more than half of global sales in China. The total number of electric cars on the road in 2017 surpassed 3 million worldwide, an expansion of over 50% from 2016. In terms of share, Norway remains the world's most advanced market for electric car sales, accounting for over 39% of new sales in 2017. Iceland follows at 11.7%, then Sweden at 6.3%. The IEA also predicted that the number of EVs on the road will reach 125 million by 2030 under the IEA's New Policies Scenario. On the other hand, the progress in CASE (connected, autonomous, shared, electrification) is expected to bring a discontinuous change in the value chain and business model of the automotive industry. It is said that this change will create opportunities and threats in the automotive market. If electrification spreads among service provider businesses, as seen in current smartphones business, it is considered that it will bring a great impact on the automobile industry. The important feature is that electric vehicles are operated by electric motors under digital control. At present, the smartphone is customized according to personal preference by downloading various applications. By comparison, electric vehicles can also be expected to customize performance such as safety, electricity cost, steering stability, and riding comfort. In the future, users will be able to download various control applications supplied from the Internet and enjoy functions that suit their personal preferences in the form of software simply by acquiring vehicles that satisfy the basic functions as a means of transportation.

Stabilization of vehicle dynamics to sudden disturbance is an important technical issue, especially for future electrification and autonomous driving [2]. However, in terms of safety and electricity costs, it should be noted that such performance controls with a large current would be associated with risks, including waste of electricity and unpredictable system malfunction. Hence, it can be considered that the part of control with these large currents should be left to the driver's operation or a safe-driving autonomous system. In this work, it was found that the steering stability of the electric vehicle was greatly improved by superimposing a small alternating current on the control current of the driver's operation to suppress the tire disturbance noise. In modern control engineering, this can be classified into intelligent control, represented by artificial intelligence (AI), and robust control, represented by disturbance suppression control. In this work, the latter was selected to achieve the stable control by repeatedly processing the signal from the sensor with higher computer processing speed. In the case of human beings, instead of using cerebral functions such as AI, reflex nerve functions prioritize response speed to avoid the risk. We thought that this idea could be applied to the tire disturbance control. We finally found that it worked very well and made it possible to suppress the disturbance of each tire independently with higher processing speed and without any cross processing between tire control command signals. In future, the direct drive in-wheel motor system will be the most suitable system for the tire digital control algorithm [3–6]. Furthermore, it will be necessary to reduce the un-sprung mass of the in-wheel motors with additional technology [7].

The dynamic response of a tire is 100-times faster than that of a vehicle body, because the weight of a tire is much less than that of a vehicle body. An electric motor also has 100-times higher mechanical response than a combustion engine [8]. The time constant of the tire lateral force, τ_{y}, can be represented by Equation (1) [9]:

$$\tau_{\mathrm{y}} = \frac{\mathrm{C}_p}{\mathrm{KV}}, \tag{1}$$

where, C_p is cornering power, K is a tire lateral stiffness, and V is a vehicle speed. Furthermore, the time constant of the longitudinal force, τ_{x}, can be represented by Equation (2) [9]:

$$\tau_{\mathrm{x}} = \frac{\mathrm{B}}{|\mathrm{u}|}, \tag{2}$$

where, B represents a relaxation length of the tire longitudinal force (travel distance required for a tire to generate a steady longitudinal force), and u represents the traveling speed of the wheel.

From Equations (1) and (2), it was calculated that τ_y = 0.001 s (C_p = 1.4 kN/deg., $K = 10^5$ N/m) and τ_x = 0.004 s (B = 0.05 m) at vehicle speed V = 50 km/h. These values are close to 0.0008 s, which is the time constant of the electric motor. This suggests that the tire and electric motor can be a good combination to achieve a quick response for a faster control system. Hence, we proposed a new concept of tire digital control, which can stabilize the vehicle dynamics by suppressing the disturbance on tires using the electric motor before the vehicle body becomes unstable. Figure 1 shows the type of control objects corresponding to control frequency range. The conventional control objects, such as anti-lock braking system (ABS) and dynamic stability control (DSC), are targeting the frequency ranges from 0.1 to 10 s. But those of tire digital control range from 1 to 100 ms, which can be achieved only by the controller of the electric-driven system. It is also an important feature that the electric motor can control both driving and braking forces. Our study showed that the tire disturbance control with electric motors, corresponding to higher frequency range, can be more effective on critical steering performances, such as those on a wet skid pad.

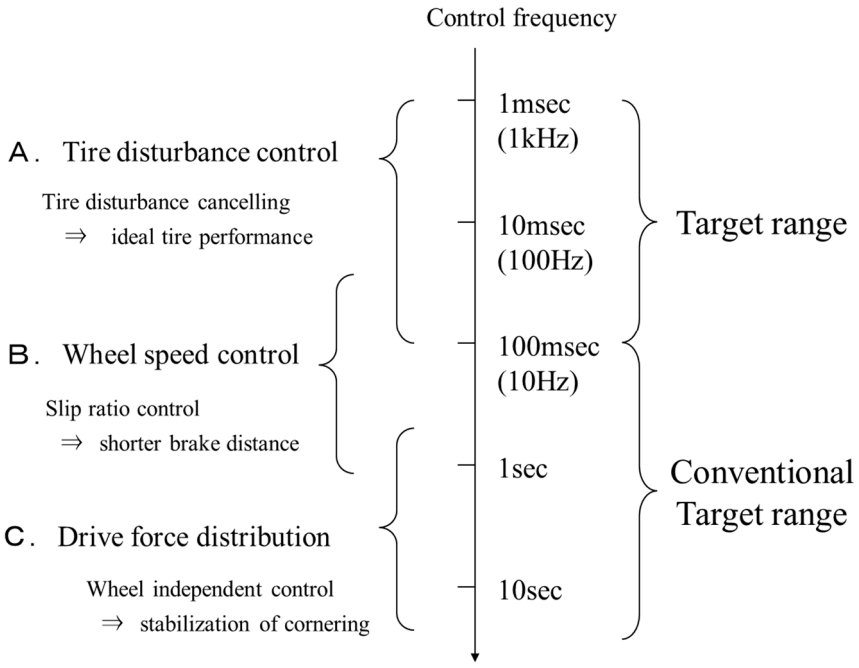

Figure 1. Control system corresponding to control frequency range.

2. Algorithm

2.1. Tire Disturbance Control

As shown in Figure 2, the tire driving force, F_d, includes the disturbance noise of the tire contact patch, $N1$, and the vibration of un-sprung mass, $N2$. The tire disturbance control can cancel out these noises by electric motor [10]. The cut-off frequency was determined so as to reduce the magnitude of transfer function of slip ratio to tire driving force, F_d/λ, between 10 Hz to 1 kHz, keeping the human maneuver frequency less than 10 Hz unaffected.

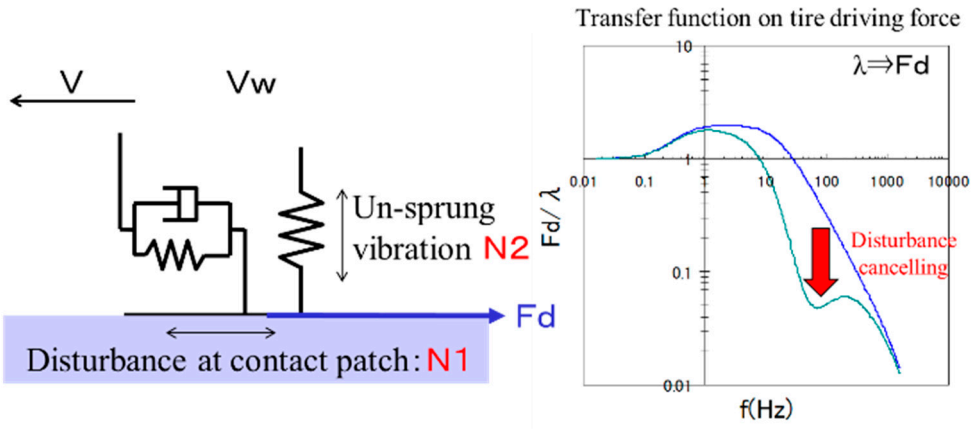

Figure 2. Design of tire disturbance controller for mechanical tire noise cancellation.

2.2. Tire Disturbance Control Algorithm

The algorithm was redesigned on the basis of the model following the control system proposed by Hori and Sakai [11]. The transfer function of the vehicle body, shown in Equation (3), was used:

$$\frac{\Delta\lambda}{\Delta F_m} = \frac{1}{\frac{d\mu}{d\lambda}\cdot F_Z}\cdot\frac{M(1-\lambda)}{M_W + M(1-\lambda)}\cdot\frac{1}{\tau_a\cdot s+1}, \quad (3)$$

where M is the vehicle weight, μ is F_d/F_z, F_d is a driving force, F_z is a load, M_w is the mass conversion value of tire inertia, V_W is the speed conversion value of tire rotational angular velocity, F_m is the motor force conversion value of torque, λ is the tire slip ratio, and s represents the Laplace operator. The time constant of the vehicle body can be given by Equation (4):

$$\tau_a = \frac{M \cdot V}{\frac{d\mu}{d\lambda} \cdot F_Z} \cdot \frac{M_W}{M_W(1-\lambda) + M(1-\lambda)^2}, \tag{4}$$

where the time constant increases as the magnitudes of M, M_w, and V increase. In addition, it should be noted that as $d\mu/d\lambda$ approaches zero at the maximum value of μ, the time constant rapidly increases and it becomes difficult for the vehicle body to respond to control. This suggests that it is necessary to stabilize the tire before the value of μ reaches the maximum value. As shown in Figure 3, the motor driving force, F_m, can be divided into the wheel inertia force, F_w, and the tire driving force, F_d, for moving forward the vehicle body. The output of F_m can be given directly from electric motor and the input of F_w can be calculated from the wheel rotation speed, V_w. The output of F_d is derived from the equation of $F_d = F_m - F_w$ as the force generated at the tire contact patch. From the comparison of F_d and the force followed by the nominal model, the abrupt slip and micro vibration at a higher frequency range was extracted by low pass filter. The component of human maneuvers was compensated by high pass filter. The filtered noise component was subtracted from the command value of F_m to be applied to the motor controller. In order to find the effective frequency pass, the cut-off frequency of low pass filter was varied from 0.01 to 10 kHz, and that of high-pass filter was varied from 0.01 to 10 Hz. The former can cut off the higher frequency disturbance noise from the electrical circuits and the latter can cut off the lower frequency disturbance noise, keeping the human maneuvers unaffected. It is important that all human maneuvers, such as throttling, braking, and handling, be kept unaffected by optimizing the cut-off frequency of low pass filter.

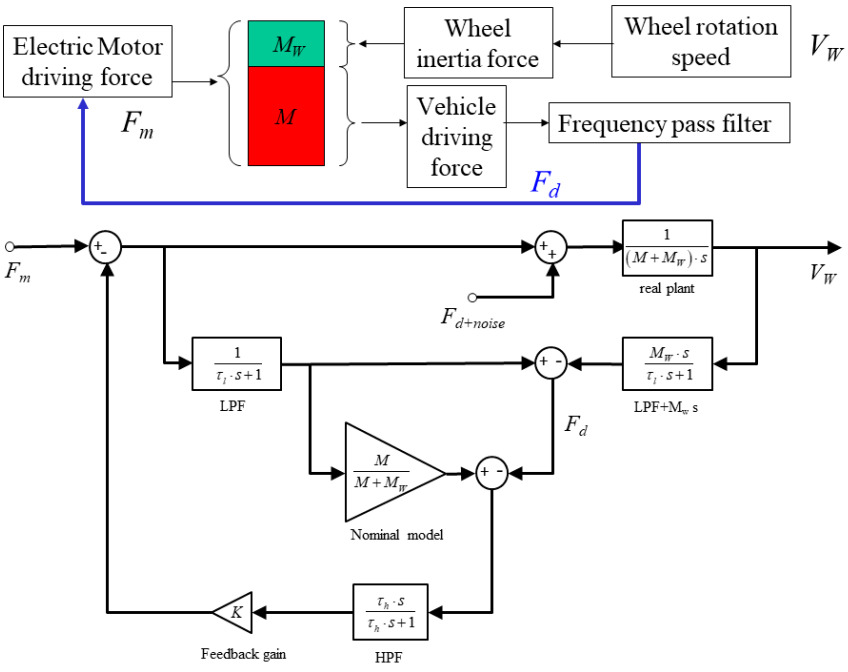

Figure 3. Design of tire disturbance controller for mechanical tire noise cancellation (LPF: low pass filter, HPF: high pass filter).

3. Results

3.1. Test Vehicle

The electric vehicle with twin motor system was constructed as a test vehicle, in which right and left rear wheels were independently controlled by two 35 kW electric motors (Figure 4). The encoder in each motor detected the rotation speed independently. The motor torque was also measured with a torque sensor attached to the motor rotating axis. Tire size on the front was 185/55R15 and 205/55R15 on the rear. In order to evaluate the instability of the vehicle dynamic behavior, the vehicle was equipped with sensors for GPS, steering angle, and yaw rate.

Figure 4. Test electric vehicle equipped with twin motor system.

3.2. Test Method

The implementation evaluation of the control system was carried out on a wet skid pad, which performed a steady turning test on the low-friction surface (Figure 5). The radius of steady turning was kept at 30 m as to find its critical turning speed by increasing turning velocity. The speed at which the amount of steering exceeded a threshold value was taken as the critical speed. The threshold value depended on the limit of the friction circle. A test driver evaluated the steering performance according to a 5-grade scoring system [12].

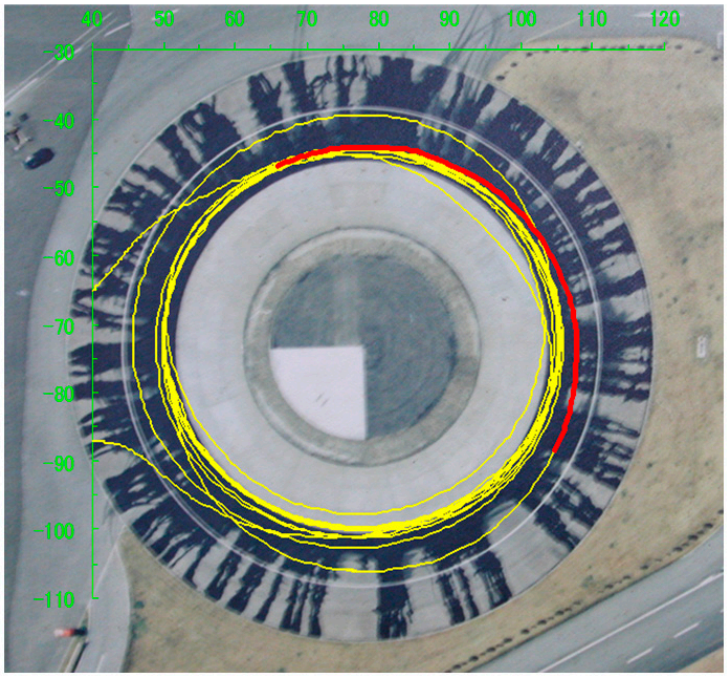

Figure 5. The aerial photo of the skid pad superimposed by the GPS trajectory of the vehicle's center of gravity.

4. Results and Discussion

4.1. Effect of Applied Control Frequency

The steering feeling at critical speed was evaluated on the wet skid pad, as shown in Figure 5. Firstly, the relationship between F_m and F_d at the steady state of the accelerated turning test was investigated and is shown in Figure 6. According to Equation (3), when the tire keeps the grip with road surface at adhesive state, F_d is proportional to F_m as shown as a straight line in Equation (5). In this state most of the motor torque can be transferred to the tire driving force:

$$F_d = \frac{M}{M + M_W} \cdot F_m, \tag{5}$$

In Figure 6 the actual force generated at the rear-right tire (RR position) as a function of the force generated by the motor was superimposed on the same graph. It can be seen that the actual measuring value of F_d followed a straight line. This shows that the tire can keep the stable grip with the road surface under the driver's control.

Figure 7 shows the relationship between F_d and F_m in the state just before the spinout. The results showed that F_d does not follow Equation (5) and fluctuates largely independent of F_m. This indicated that the tire already showed signs of spinout just before the vehicle spinout and suggested that it is possible to expand the stability margin by suppressing this fluctuation by motor control.

The ranges of the tire digital control frequency were determined by the combinations of cut-off frequencies of high pass and low pass filter: I: 10–1000 Hz, II: 1–100 Hz, III: 0.1–10 Hz, IV: 0.01–1 Hz, and V: 0.01–1000 Hz. The magnitude of the effect is shown in Figure 8 together with the corresponding evaluation score of steering feeling. The rating was evaluated with the highest score of 7 and the lowest score of 5, according to the 5-grade system. The evaluation was carried out as a relative evaluation method with a reference of without control [12]. It was confirmed that the score of steering feeling increased with increasing control frequency. The best frequency range was found to be from 10 to 1000 Hz, which corresponded to the length scale per control cycle from 1 m to 1 cm on the tire circumference at a speed of 40 km/h. The length scale of 1 m and 1 cm corresponded to the half-length

of the tire circumference and that of a piece of block pattern on the tire tread rubber, respectively. The most frequent control length within this range can correspond to the tire contact patch length of around 10 cm. The most effective control frequency range at critical driving on the wet skid pad was found to correspond close to the tire scale length. It was, hence, proved that the tire digital control can be completed within the tire scale length.

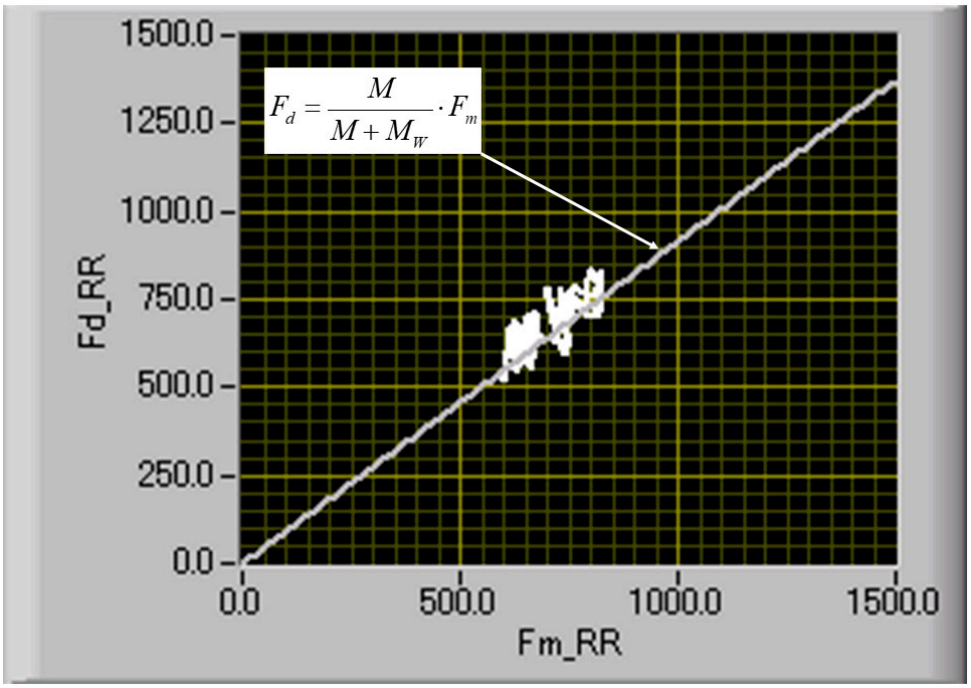

Figure 6. Relationship between the friction force, F_{d_RR}, and the motor torque, F_{m_RR}, at steady state in the accelerated turning test.

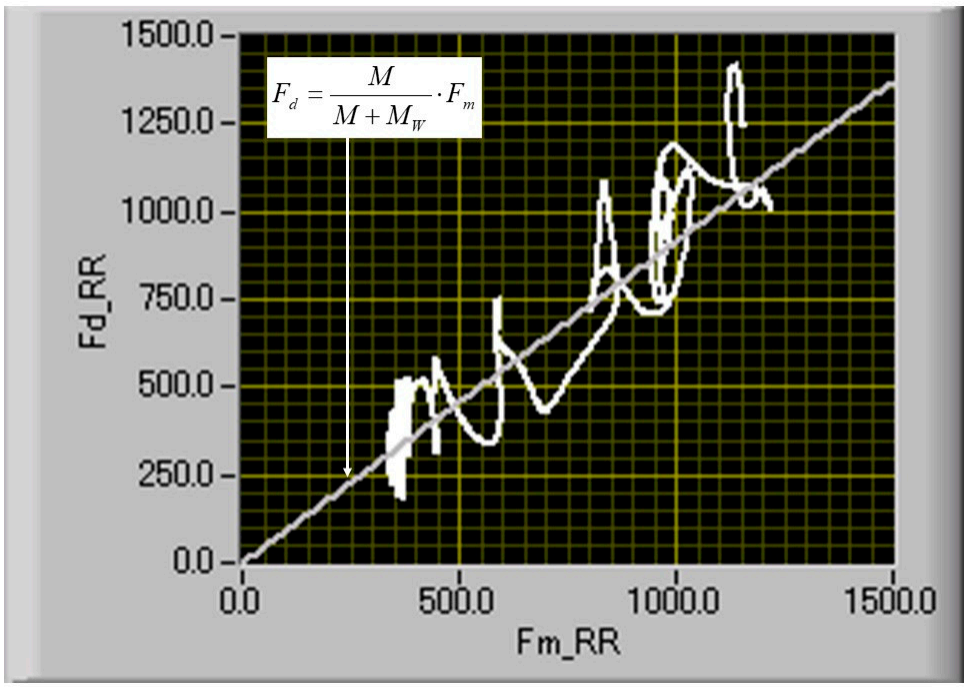

Figure 7. Relationship between friction force, F_{d_RR}, and motor torque, F_{m_RR}, just before the spinout in the accelerated turning test.

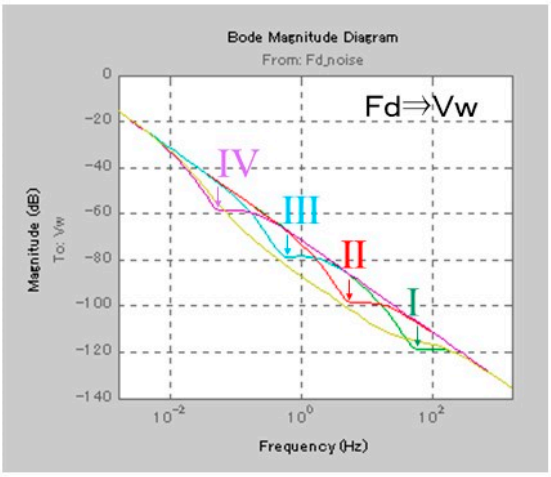

Frequency range	score
w/o control	5
I	7
II	6. 5
III	6
IV	5. 5
I−IV	7

Figure 8. The magnitude of the effect on each control frequency range and the corresponding score of steering feeling.

4.2. Stabilization of Steering on the Wet Skid Pad

The effect of tire digital control on the stabilization of vehicle dynamics was examined quantitatively by on-board sensors measuring the steering angle (deg) and the yaw rate (deg/sec). It was compared with those examined without the tire digital control. The cut-off frequency of 10–1000 Hz was chosen as the most effective frequency band. The radius of turning was kept at 30 m on the wet skid pad, increasing its vehicle speed up to the critical speed. The steering performance charts, represented by the plot of yaw rate (deg/sec) against steering angle (deg) at the critical speed, are shown in Figure 9. The critical speed with the tire digital control was 45 km/h and without control was 44 km/h.

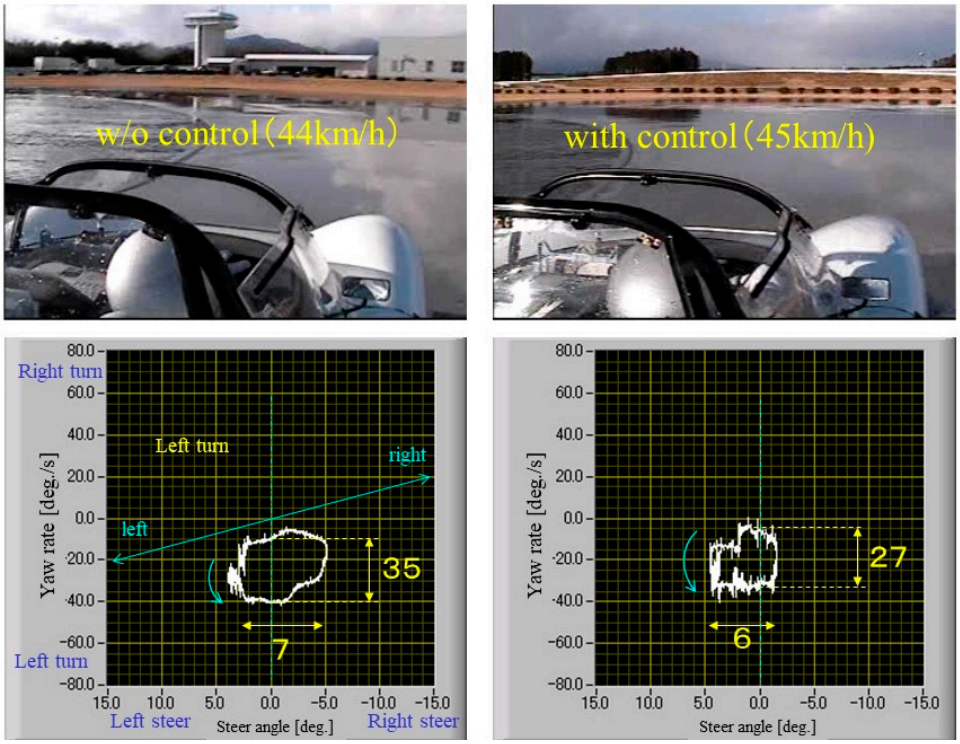

Figure 9. Steering maneuvering on the wet skid pad compared between vehicles with and without the tire digital control. More details can be found in Supplementary Materials (Video S1: without control and Video S2: with control).

The steering characteristics were determined by the deviation from the centerline at the zero steer angle on the chart. The stability of the vehicle was estimated from the size and position of the hysteresis loop on this chart. As the vehicle speed became close to the critical speed, the vertical loads on the outer side of tires became higher and those on the inner side of the tires became lower on average. Both of the tire grips became unstable at the critical speed and generated stick-slip vibrations. In this situation, the tire disturbance noise could induce abrupt slip in tire contact patch, and the risk of losing maneuverability and spinout increases. When the steering characteristic suddenly changed to unstable states, the tire digital controller could suppress the abrupt slip and micro vibration generated between the tire and the road surface. This led to optimizing the distribution of driving forces of the right and left rear tires independently so as to change the steering characteristics to under-steering (U/S), thereby keeping the turning speed higher while suppressing the risk of spinout. As shown in the right figure in Figure 9, the hysteresis loop with the tire digital control appeared almost in the left steer angle area, which represents the over-steering (O/S) characteristic. This suggests that the tire digital control can stabilize the vehicle dynamics, even if it is at the over-steering (O/S) characteristic. It can be also seen that the size of the loop with the control was smaller than that without the control. This shows the fact that the driver did not have to do unnecessary steering maneuvers to avoid spinout. It should be noted that the tire digital control with the electric motor could detect and remove the abrupt slip and vibrations generated in the contact patch independently for each tire. It was, hence, concluded that the tire digital control works well on each tire independently, because it can suppress the fluctuation of each tire before the vehicle body starts to slide. This means that it does not need any information from the sensors on the vehicle body and any cooperative control between tires.

5. Conclusions

Tires are the only part that contact and interact with the road surface. Hence, we proposed a concept of the tire digital control with electric motors, which can detect and remove the disturbance noises, such as abrupt slips and vibrations, in the tire contact patch before the vehicle body becomes unstable. This also gives us the benefit that it consumes less energy than controlling a vehicle body 100-times heavier. The tire disturbance control algorithm was implemented on an electric vehicle with twin motor system and was found to be effective, especially at critical speed on a low friction road surface. The magnitude of the effect was evaluated from both steering feeling and on-board instruments. The tire disturbance algorithm can make the tire more responsive to abrupt change and the vibrations. The most effective frequency range was found to be between 10 to 1000 Hz, which corresponded to the half-length of the tire circumference and the length of a piece of block on the tread pattern, respectively. The most frequent control length can correspond to the tire contact patch length of around 10 cm. Accordingly, the road holding performance of each tire was improved and the steering stability of the vehicle can be improved. Each tire equipped with an electric motor can detect and remove the disturbance in tire contact patch independently, just like artificial intelligence, and stabilize the vehicle dynamics, especially at critical speed on a low friction surface.

Supplementary Materials: The following are available online at http://www.mdpi.com/2032-6653/10/2/25/s1. Video S1: without control and Video S2: with control.

Author Contributions: Investigation, K.A. and Y.W.

Funding: This research received no external funding.

Acknowledgments: The authors would like to thank Bridgestone Corporation to permit the publishing of this paper. Grateful acknowledgement is made to Y. Hori at the University of Tokyo for useful discussions and advice to start thinking of the tire disturbance control algorithm on this project.

Conflicts of Interest: The authors declare no conflict of interest.

References

1. Global Electric Vehicle (EV) Outlook 2018. Available online: https://www.iea.org/gevo2018/ (accessed on 15 April 2019).
2. Anderson, Z.M.; Glovanardi, M.; Tucker, C.; Ekehian, J.A. Active Safety Suspension System. US2017/0137023, 18 May 2017.
3. Wang, Y.; Fujimoto, H.; Hara, S. Driving Force Distribution and Control for EV with Four In-Wheel Motors: A Case Study of Acceleration on Split-Friction Surfaces. *IEEE Trans. Ind. Electron.* **2016**, *64*, 3380–3388. [CrossRef]
4. Nam, K.; Oh, S.; Fujimoto, H.; Hori, Y. Estimation of Sideslip and Roll Angles of Electric Vehicles Using Lateral Tire Force Sensors Through RLS and Kalman Filter Approaches. *IEEE Trans. Ind. Electron.* **2012**, *60*, 988–1000. [CrossRef]
5. Hu, J.; Wang, Y.; Fujimoto, H.; Hori, Y. Robust Yaw Stability Control for In-wheel Motor Electric Vehicles. *IEEE/ASME Trans. Mechatron.* **2017**, *22*, 1360–1370. [CrossRef]
6. Sato, M.; Yamamoto, G.; Gunji, D.; Imura, T.; Fujimoto, H. Development of Wireless In-Wheel Motor Using Magnetic Resonance Coupling. *IEEE Trans. Power Electron.* **2016**, *31*, 5270–5278. [CrossRef]
7. Nagaya, G.; Wakao, Y.; Abe, A. Development of an in-wheel drive with advanced dynamic-damper mechanism. *JSAE Rev.* **2003**, *24*, 477–481. [CrossRef]
8. Hori, Y.; Toyoda, Y.; Tsuruoka, Y. Traction Control of Electric Vehicle: Basic Experimental Results using the Test EV UOT Electric March. *IEEE Trans. Ind. Appl.* **1998**, *34*, 1131–1138. [CrossRef]
9. Clark, S.K. *Mechanics of Pneumatic Tires*; Chapter 9, Analysis of tire properties; National Highway Traffic Safety Administration: Washington, DC, USA, 1981; pp. 721–757.
10. Wakao, Y.; Akutagawa, K. Method And Device For Controlling Vehicle. EP1502805A1, 2 February 2005.
11. Hori, Y.; Sakai, S.; Sado, H.; Uchida, T. Motion Control of Electric Vehicle Utilizing Fast Torque Response of Electric Motor. *IFAC Proc. Vol.* **1999**, *32*, 8166–8171. [CrossRef]
12. Nasukawa, K.; Miyashita, Y.; Shiokawa, M. Jidousha No Soukouseinou To Shikenhou. In *Efficiency Tests for Running*, 3rd ed.; Sankaido: Tokyo, Japan, 1993; p. 217.